

Testing the higgsino-singlino sector of the NMSSM with trileptons at the LHC

Ulrich Ellwanger

Laboratoire de Physique Théorique, UMR 8627,
CNRS and Université de Paris–Sud, F-91405 Orsay, France

Abstract

We propose a simplified light higgsino-singlino scenario in the NMSSM, in which the masses of the chargino and the lightest neutralino determine the masses and couplings of all 3 lightest neutralinos. This scenario is complementary to the simplified wino-like chargino/neutralino scenario used conventionally for the interpretation of results from trilepton searches, and motivated by lower bounds on the gluino mass in the case of GUT relations between the wino and gluino masses. We present all masses and mixing angles necessary for the determination of production cross sections of the chargino and the 3 neutralinos in the form of Tables in the $M_{\chi_1^0} - M_{\chi_1^\pm}$ plane, assuming Higgs mass motivated values for $\tan\beta = 2$ and $\lambda = 0.6$. We show that this scenario leads to considerable signal rates, and present constraints in this plane from recent searches for trileptons at the LHC.

1 Introduction

One of the main tasks of the LHC is the search for supersymmetric (SUSY) particles. These searches have been without success so far, and have lead to lower bounds in the TeV range on the masses of gluinos and squarks of the first two generations.

The trilepton channel $pp \rightarrow W^{(*)} \rightarrow \chi^\pm + \chi_i^0$ ($i > 1$) with $\chi^\pm \rightarrow W^{(*)} + \chi_1^0$, $\chi_i^0 \rightarrow Z^{(*)} + \chi_1^0$ and leptonic decays of both $W^{(*)}$ and $Z^{(*)}$ are considered as “gold-plated” for searches for charginos and neutralinos at hadron colliders [1–9]. Corresponding searches at the LHC using leptonic final states, in particular trileptons plus missing transverse energy, have been performed by ATLAS and CMS [10–15]; see [16,17] for recent results from trilepton searches at $\sqrt{s} = 8$ TeV. There, the absence of significant excesses of events is interpreted in simplified models, motivated by the SUSY particle content of the Minimal SUSY extension of the Standard Model (MSSM) and assuming simple branching ratios and relations among masses. Interpretations of the present constraints from the trilepton channel in realistic versions of the MSSM have been performed in [18–21] (see [22–24] for the rôle of trilepton final states in some beyond-the-MSSM models).

A particularly challenging MSSM scenario would be the case of light and nearly degenerate higgsinos [25, 26]. Light higgsinos correspond to a relatively small ($\lesssim 300$ GeV) SUSY Higgs mass parameter μ , which is favored by fine-tuning arguments: μ^2 appears always as a positive mass² parameter in the Higgs potential, and must be compensated by negative soft SUSY breaking Higgs mass terms for electroweak symmetry breaking to be possible. This makes large values of μ unnatural, since then the required cancellation must be relatively very precise. On the other hand, a dominantly higgsino-like (neutralino) LSP is a difficult candidate for dark matter: its annihilation cross section in the early universe is typically too large so that, assuming a standard cosmological evolution, its relic density today is too small to comply with the WMAP and Planck result $\Omega h^2 \sim 0.1187$. Moreover, its direct detection (nucleon) cross section is also too large [21, 27] in view of the latest XENON100 results [28] unless the higgsino component is close to 100%.

In the Next-to-Minimal Supersymmetric Standard Model (NMSSM) [29], a SUSY Higgs mass parameter μ_{eff} is generated dynamically through the vacuum expectation value (vev) of a gauge singlet superfield S , $\mu_{\text{eff}} = \lambda \langle S \rangle$, where λ denotes the coupling of S to the MSSM-like Higgs superfields. Again, small values of μ_{eff} are favored by low fine-tuning [30,31]. However, the problems associated with a higgsino-like LSP in the MSSM do not persist in the NMSSM due to the presence of the additional neutralino (singlino) from the superfield S , which can well be lighter than the higgsinos. This allows for a dominantly singlino-like LSP, whose annihilation cross section via Higgs bosons in the s-channel (and/or coannihilation or some higgsino component) can lead to the desired relic density (see [29] and refs. therein), and a sufficiently small direct detection cross section [32–35] compatible with present XENON100 bounds.

Hence a scenario with light higgsinos and a light singlino, but heavy electroweak gauginos, is viable in the NMSSM. Assuming GUT relations among the electroweak gauginos and the gluino, heavy electroweak gauginos would be an obvious consequence of lower bounds well above 1 TeV on the gluino mass. Since higgsino-singlino mixing would lift the degeneracy among the neutral and charged higgsinos and in the presence of a light singlino-like LSP, searches for charginos and neutralinos in the trilepton channel would be more promising

than in the light higgsino scenario within the MSSM [25].

We emphasize that such a scenario would be complementary to the simplified models used by ATLAS and CMS for the interpretation of the trilepton results up to now: In these models, the lightest chargino and the second lightest neutralino are assumed to be wino-like and degenerate, the lightest neutralino is assumed to be bino-like, and the higgsinos are assumed to be heavy and decoupled. The obvious reason for this choice is that now signal rates depend on only two mass parameters (assuming 100% branching ratios into $W/Z + \chi_1^0$).

In the light higgsino-singlino scenario of the NMSSM (containing one chargino χ_1^\pm and 3 neutralinos χ_i^0 , $i = 1, 2, 3$) the masses and neutralino mixing angles depend on the higgsino mass parameter μ_{eff} , the singlino mass, the ratio $\tan\beta$ of Higgs vevs and the coupling λ (see the next Section). The value of ~ 125 GeV for the SM-like Higgs mass can be obtained naturally in the NMSSM provided λ is large (≈ 0.6) and $\tan\beta$ is relatively small (≈ 2) [23, 36–58]. Fixing $\tan\beta = 2$ and $\lambda = 0.6$, also the light higgsino-singlino scenario of the NMSSM depends on two mass parameters only. These can be chosen as the physical chargino mass $M_{\chi_1^\pm}$ ($\sim \mu_{\text{eff}}$) and the LSP mass $M_{\chi_1^0}$, which have a more direct physical meaning than the higgsino and singlino mass parameters in the Lagrangian.

Assuming heavy sleptons, the chargino χ_1^\pm decays with a branching ratio (BR) of 100% into $W^{(*)} + \chi_1^0$. The neutralinos $\chi_{2,3}^0$ will typically decay with a BR of 100% into $Z^{(*)} + \chi_1^0$. In some cases, decays $\chi_{2,3}^0 \rightarrow \chi_1^0 +$ a CP-odd or CP-even Higgs boson are possible. These depend on the masses and couplings of the Higgs bosons. Subsequently we define a simplified light higgsino-singlino scenario within which such neutralino-to-Higgs decays are absent. Then, given the above values of $\tan\beta$ and λ , $M_{\chi_1^\pm}$ and $M_{\chi_1^0}$ determine completely the signal rates for chargino + neutralino production into trilepton final states.

It would be very helpful if the ATLAS and CMS collaborations would interpret their results from trilepton searches within such a light higgsino-singlino scenario, as it would allow to test a well motivated region in the parameter space of the NMSSM. It also allows to generalize in a well defined manner the (somewhat unrealistic) assumption $M_{\chi_1^\pm} = M_{\chi_2^0}$ within the present simplified models, and to study the impact of the lift of this degeneracy.

In the present paper we present the necessary parameters for the determination of the $pp \rightarrow \chi_1^\pm + \chi_{2,3}^0$ production rates in the light higgsino-singlino scenario in the form of Tables in the $M_{\chi_1^\pm} - M_{\chi_1^0}$ plane: The masses $M_{\chi_2^0}$ and $M_{\chi_3^0}$ of the two additional neutralinos, and the mixing angles of χ_2^0 and χ_3^0 (relevant for the $W - \chi_1^\pm - \chi_{2,3}^0$ couplings). As a (preliminary) application we simulated the trilepton event rates in the various signal channels defined in [16], and deduced bounds in the $M_{\chi_1^\pm} - M_{\chi_1^0}$ plane from the upper limits on the corresponding channel-specific signal cross sections based on 21 fb^{-1} integrated luminosity at $\sqrt{s} = 8$ TeV given there. The Tables should allow the ATLAS and CMS collaborations to perform more precise simulations (in particular of the detector responses) and comparisons with data themselves, notably with future data at larger \sqrt{s} and/or different signal channels.

In the next Section we define the simplified light higgsino-singlino scenario in the NMSSM, and comment on the Tables given in the Appendix. In Section 3 we describe the simulations of the trilepton final states and show the resulting bounds in the $M_{\chi_1^\pm} - M_{\chi_1^0}$ plane. Section 4 is devoted to conclusions and an outlook.

2 The Light Higgsino-Singlino Scenario in the NMSSM

The NMSSM differs from the MSSM due to the presence of the gauge singlet superfield \hat{S} . In the simplest realisation of the NMSSM, the SUSY $\mu\hat{H}_u\hat{H}_d$ Higgs mass term in the MSSM superpotential W_{MSSM} is replaced by the coupling λ of \hat{S} to \hat{H}_u and \hat{H}_d , and a self-coupling $\kappa\hat{S}^3$. Here, \hat{H}_u couples to up-type quark superfields, and \hat{H}_d to down-type quark and lepton superfields. In this version the superpotential W_{NMSSM} is scale invariant, and given by:

$$W_{\text{NMSSM}} = \lambda\hat{S}\hat{H}_u \cdot \hat{H}_d + \frac{\kappa}{3}\hat{S}^3 + \dots \quad (1)$$

where the dots denote the Yukawa couplings of \hat{H}_u and \hat{H}_d to the quarks and leptons as in the MSSM. Once the scalar component of \hat{S} develops a vev s , the first term in W_{NMSSM} generates an effective μ -term with

$$\mu_{\text{eff}} = \lambda s . \quad (2)$$

Amongst others, μ_{eff} generates a Dirac mass term $\mu_{\text{eff}}\psi_u\psi_d + \text{h.c.}$ for the SU(2)-doublet higgsinos ψ_u and ψ_d . The vevs v_u and v_d of \hat{H}_u and \hat{H}_d generate mixing terms between the singlino ψ_S and ψ_d , ψ_u , respectively. The second term in the superpotential W_{NMSSM} (1) generates a Majorana mass term M_S for ψ_S with

$$M_S = 2\kappa s \equiv \frac{2\kappa}{\lambda}\mu_{\text{eff}} . \quad (3)$$

The soft SUSY breaking terms include, amongst others, mass terms for the gauginos \tilde{B} (bino), \tilde{W}^a (winos) and \tilde{G}^a (gluinos):

$$-\mathcal{L}_{1/2} = \frac{1}{2} \left[M_1 \tilde{B}\tilde{B} + M_2 \sum_{a=1}^3 \tilde{W}^a \tilde{W}_a + M_3 \sum_{a=1}^8 \tilde{G}^a \tilde{G}_a \right] + \text{h.c.} . \quad (4)$$

Altogether the symmetric 5×5 mass matrix \mathcal{M}_0 in the neutralino sector in the basis $\psi^0 = (-i\tilde{B}, -i\tilde{W}^3, \psi_d^0, \psi_u^0, \psi_S)$ is given by [29]

$$\mathcal{M}_0 = \begin{pmatrix} M_1 & 0 & -\frac{g_1 v_d}{\sqrt{2}} & \frac{g_1 v_u}{\sqrt{2}} & 0 \\ & M_2 & \frac{g_2 v_d}{\sqrt{2}} & -\frac{g_2 v_u}{\sqrt{2}} & 0 \\ & & 0 & -\mu_{\text{eff}} & -\lambda v_u \\ & & & 0 & -\lambda v_d \\ & & & & M_S \end{pmatrix} \quad (5)$$

leading to mass terms in the Lagrangian of the form

$$\mathcal{L} = -\frac{1}{2}(\psi^0)^T \mathcal{M}_0(\psi^0) + \text{h.c.} . \quad (6)$$

In the limit of heavy decoupled winos and bino considered here, $M_{1,2} \gg (\mu_{\text{eff}}, 2|\kappa s|)$ (we assume $\mu_{\text{eff}} > 0$), the light higgsino-singlino sector is described by the lower 3×3 sub-matrix $\mathcal{M}_0^{(3)}$ of (5). Besides μ_{eff} and M_S , the elements of $\mathcal{M}_0^{(3)}$ depend on λ and $\tan\beta = \frac{v_u}{v_d}$ via

$v_u = \sin \beta \sqrt{v_u^2 + v_d^2} = \sin \beta (174 \text{ GeV})$, $v_d = \cos \beta \sqrt{v_u^2 + v_d^2}$. As stated in the introduction, we define subsequently the simplified light higgsino-singlino scenario by $\lambda = 0.6$, $\tan \beta = 2$.

$\mathcal{M}_0^{(3)}$ is diagonalized by an orthogonal real matrix N_{ij} , $i = 1, 2, 3$, $j = 3, 4, 5$ such that the physical masses $M_{\chi_i^0}$ ordered in $|M_{\chi_i^0}|$ are real, but not necessarily positive. Denoting the 3 eigenstates by χ_i^0 , we have

$$\chi_i^0 = N_{ij} \psi_j^0 \quad (7)$$

where $\psi_3^0 = \psi_d^0$, $\psi_4^0 = \psi_u^0$, $\psi_5^0 = \psi_S$.

The Dirac mass $M_{\chi_1^\pm}$ of the higgsino-like charginos χ_1^\pm is simply $M_{\chi_1^\pm} = \mu_{\text{eff}}$.

The calculations of the masses and mixing angles as function of the parameters λ , κ (which determines M_S), μ_{eff} and $\tan \beta$ are performed with the help of the public code **NMSSM-Tools** [59, 60]. Due to the radiative corrections to the pole masses, $M_{\chi_1^\pm}$ differs slightly from μ_{eff} . For the soft SUSY breaking squark and slepton masses we choose 2 TeV, and $M_1 = 1 \text{ TeV}$, $M_2 = 2 \text{ TeV}$, $M_3 = 6 \text{ TeV}$. (These SUSY breaking parameters determine implicitly the SUSY breaking scale which has a mild impact on the radiative corrections.)

The soft SUSY breaking parameters A_λ and A_κ [29] have no impact on the neutralino/-chargino sector. They can be chosen such that the SM-like Higgs mass is near 125 GeV; in any case they must be chosen such that all physical Higgs masses² are positive.

Subsequently we consider $M_{\chi_1^\pm}$ in the range $M_{\chi_1^\pm} = 100 \dots 400 \text{ GeV}$ in steps of 20 GeV. The corresponding values of μ_{eff} are tabulated in Table 1 in the Appendix.

For $M_{\chi_1^0}$ we consider the range $M_{\chi_1^0} = 0 \dots 100 \text{ GeV}$ in steps of 10 GeV. For fixed λ , $\tan \beta$ and for each given μ_{eff} , the desired values for $M_{\chi_1^0}$ can be obtained by suitable values of κ . Actually, low values of $M_{\chi_1^0}$ require negative values for κ (we recall that we assume $\mu_{\text{eff}} > 0$). Along a strip around $\kappa \sim 0$, negative and positive values of κ (of different absolute values) can lead to the same values of $M_{\chi_1^0}$. We chose the convention $\kappa > 0$ whenever possible, which lifts this ambiguity. The corresponding values for κ are tabulated in Table 2 in the Appendix. Note that $M_{\chi_1^0} = M_{\chi_1^\pm} (= 100 \text{ GeV})$ is not possible for $M_S \leq \mu_{\text{eff}}$ as considered here, since even for $M_S = \mu_{\text{eff}}$ mixing in the neutralino sector will always imply $M_{\chi_1^0} < M_{\chi_1^\pm}$ (by at least 3 GeV).

Now the masses and mixing angles of χ_2^0 and χ_3^0 are uniquely determined. In the Tables 3 and 4 in the Appendix we list $M_{\chi_2^0}$ and $M_{\chi_3^0}$ in the considered range of $M_{\chi_1^\pm}$ and $M_{\chi_1^0}$. We see that $M_{\chi_2^0}$ is close to $M_{\chi_1^\pm} \sim \mu_{\text{eff}}$, whereas $M_{\chi_3^0}$ is significantly larger due to mixing. (For $M_{\chi_1^0} \gtrsim M_{\chi_1^\pm} - 20 \text{ GeV}$ in the lower left-hand corner, the mixing angles differ considerably from the other part of the plane.)

The mixing angles $N_{i,j}$ with $i = 2, 3$, $j = 3, 4$ appear in the Feynman rule for the vertex in $W^+ \rightarrow \chi_1^+ + \chi_{2,3}^0$ corresponding to an incoming W_μ^+ , an outgoing higgsino-like chargino χ_1^+ and outgoing neutralinos $\chi_{2,3}^0$; the projectors P_L , P_R act on the neutralino 4-spinors:

$$ig_2 \gamma_\mu (N_{i,3} P_R - N_{i,4} P_L) / \sqrt{2}. \quad (8)$$

Note that the last factor $1/\sqrt{2}$ is absent in the coupling of W to wino-like charginos and neutralinos (not shown here); as a consequence the production rates of higgsino-like charginos and neutralinos considered here are smaller than those of wino-like charginos and neutralinos assumed in the simplified models used by ATLAS and CMS. The mixing angles $N_{2,3}$, $N_{2,4}$, $N_{3,3}$ and $N_{3,4}$ are tabulated in the Tables 5, 6, 7 and 8, respectively, in the Appendix. Since

the signs of physical spinors can be flipped without affecting the cross sections, we used this freedom to simplify the tables in the lower left-hand corner where frequent sign changes appear as consequence of the numerical diagonalisation routine.

Given the decoupled winos and bino, the (absolute values of) the singlino components of χ_i^0 , $i = 2, 3$, are given by $|N_{i,5}| = \sqrt{1 - N_{i,3}^2 - N_{i,4}^2}$, and are typically quite small with the exception of $N_{3,5}$ for $M_{\chi_1^0} \lesssim M_{\chi_1^\pm}$ (in the lower left-hand corner of the Tables). Likewise, the (absolute values of) the higgsino components $N_{1,i}$ ($i = 3, 4$) of χ_1^0 are given by $|N_{1,i}| = \sqrt{1 - N_{2,i}^2 - N_{3,i}^2}$, from which the singlino component $N_{1,5}$ of χ_1^0 (typically dominant) can be deduced as before.

Assuming BRs of 100% for the decays $\chi_2^0 \rightarrow Z^{(*)} + \chi_1^0$, $\chi_3^0 \rightarrow Z^{(*)} + \chi_1^0$ and $\chi_1^\pm \rightarrow W^{(*)} + \chi_1^0$, the masses and the $W - \chi_1^\pm - \chi_{2,3}^0$ vertices suffice to determine the production cross sections and signal rates into trilepton channels in this light higgsino-singlino scenario. Hence this scenario is now well defined (on the points given in the Tables), and can be used to interpret results from searches for trileptons and missing energy. If desired, the parameters of additional points in the $M_{\chi_1^0} - M_{\chi_1^\pm}$ plane can be provided.

3 Present LHC Constraints on the Light Higgsino-Singlino Scenario

Recent results from searches for trileptons and missing energy at the LHC at $\sqrt{s} = 8$ TeV and $\sim 20 \text{ fb}^{-1}$ of integrated luminosity have been published in [16, 17]. Subsequently we use the upper bounds (at the 95% confidence level) on event rates in the specific search channels given by ATLAS in the Table 1 in [16]. For the simulation we proceed as follows:

The cross sections for $pp \rightarrow \chi_1^\pm + \chi_2^0$ and $pp \rightarrow \chi_1^\pm + \chi_3^0$ production are obtained from Prospino at next-to-leading order (NLO) [61–63]. The matrix elements are generated by MadGraph/MadEvent 5 [64], which includes Pythia 6.4 [65]. The output is given to the fast detector simulation DELPHES [66, 67]. We have verified that the cut flows given in Table 5 in [16] are reproduced reasonably well (within 10 – 30%).

The strongest constraints on the light higgsino-singlino scenario originate from the search channels SRnoZc and SRZc in [16], which are defined as follows: m_{SFOS} denotes the invariant mass of a same-flavour opposite-sign (SFOS) lepton pair (closest to the Z -boson mass). For SRnoZc one requires $m_{\text{SFOS}} < 81.2$ GeV or $m_{\text{SFOS}} > 101.2$ GeV, whereas for SRZc one requires $81.2 \text{ GeV} < m_{\text{SFOS}} < 101.2 \text{ GeV}$. For p_T^l of the third leading lepton one requires $p_T^l > 30$ GeV for SRnoZc, and $p_T^l > 10$ GeV for SRZc. For the missing transverse energy E_T^{miss} one requires $E_T^{\text{miss}} > 75$ GeV for SRnoZc, and $E_T^{\text{miss}} > 120$ GeV for SRZc. The transverse mass m_T is defined by $m_T = \sqrt{2 \cdot E_T^{\text{miss}} \cdot p_T^l \cdot (1 - \cos \Delta\Phi_{l, E_T^{\text{miss}}})}$, and required to be above 110 GeV in all cases. The upper bounds on the number of signal events are 6.8 for SRnoZc, and 6.5 for SRZc (for more details, see [16]).

The resulting constraints in the $M_{\chi_1^0} - M_{\chi_1^\pm}$ plane are shown as a red curve in Fig. 1. The black dashed line in Fig. 1 indicates where $M_{\chi_2^0} - M_{\chi_1^0} = M_Z$. Above the black dashed line, χ_2^0 (with a significantly larger production cross section than χ_3^0) undergoes 3-body decays $\chi_2^0 \rightarrow \chi_1^0 + Z^* \rightarrow \dots$, and the search channel SRnoZc is most relevant, whereas below the

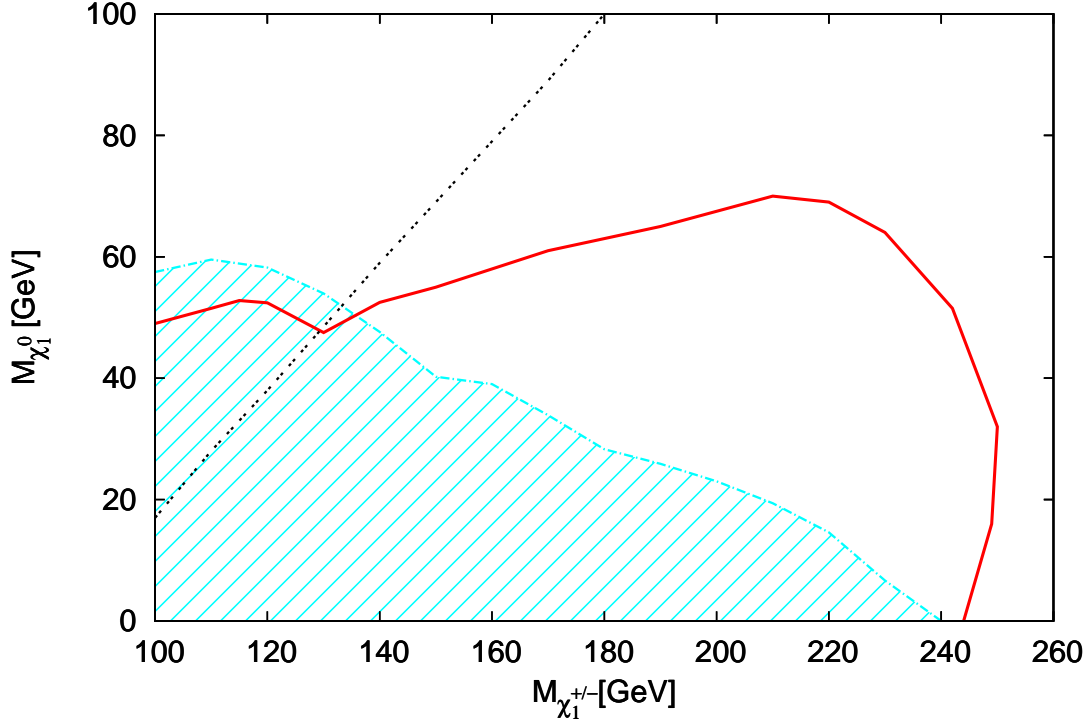


Figure 1: Red curve: Boundary of the excluded region in the $M_{\chi_1^0} - M_{\chi_1^\pm}$ plane from searches for trileptons by ATLAS [16]. The black dashed line indicates $M_{\chi_2^0} - M_{\chi_1^0} = M_Z$. Above the black dashed line, χ_2^0 undergoes 3-body decays $\chi_2^0 \rightarrow \chi_1^0 + Z^* \rightarrow \dots$. The blue hashed region is excluded by searches for $\chi_2^0 + \chi_1^0$ production at LEP [68, 69].

black dashed line χ_2^0 undergoes 2-body decays $\chi_2^0 \rightarrow \chi_1^0 + Z \rightarrow \dots$, and the search channel SRZc is relevant.

We note that the bounds in the $M_{\chi_1^0} - M_{\chi_1^\pm}$ plane are significantly weaker than the bounds in Fig. 8(b) in [16]. The reason herefore is the significantly lower production cross section for higgsino-like charginos and neutralinos compared to wino-like charginos and neutralinos assumed in the simplified model in [16]. The fact that here we include in addition the production of χ_3^0 does not compensate for the smaller couplings to W^* (also due to mixings with the singlino), moreover $M_{\chi_3^0}$ is substantially larger than $M_{\chi_2^0}$.

Searches for $e^+e^- \rightarrow Z^{(*)} \rightarrow \chi_2^0\chi_1^0$ had already been performed at LEP, notably by the DELPHI [68] and OPAL [69] collaborations. Since the $Z - \chi_2^0 - \chi_1^0$ vertex is equally well defined in the present scenario, corresponding constraints (as implemented in `NMSSMTools` [59, 60]) can be applied and lead to the excluded blue hashed region in Fig. 1. Actually, inside the blue hashed region (for $M_{\chi_1^0} < M_Z/2$ and low $M_{\chi_1^\pm}$ where the higgsino components of χ_1^0 are not negligibly small), some points are also excluded by a too large contribution to the invisible Z width from $Z \rightarrow \chi_1^0\chi_1^0$.

Hence, even in this somewhat delicate light higgsino-singlino scenario, already the present LHC constraints are significantly stronger than the bounds from LEP.

4 Conclusions and outlook

The main purpose of the present paper is the presentation of a simplified, but well-motivated light higgsino-singlino scenario in the NMSSM. It is complementary to the simplified wino-like chargino/neutralino scenario used conventionally by ATLAS and CMS for the interpretation of results from trilepton searches, but leads equally to considerable signal rates. (Assuming GUT-like relations among the gaugino mass parameters, the wino mass term is bounded from below by about 1/3 of the lower limit on the gluino mass, disfavoured light winos.) Hence present and future searches for chargino/neutralino production at the LHC merit to be interpreted in this scenario as well.

We have presented all necessary masses and mixing angles for the determination of production cross sections of the chargino and the 3 neutralinos in the form of Tables in the $M_{\chi_1^0} - M_{\chi_1^\pm}$ plane, assuming Higgs mass motivated values (in the NMSSM) for $\tan\beta = 2$ and $\lambda = 0.6$; however, as long as λ remains sizeable and $\tan\beta$ small, the masses and mixing angles depend little on these specific values. Masses and mixing angles for additional points in this plane can be provided by the author, or be obtained with the help of the public code `NMSSMTools` [59, 60].

The present constraints in the $M_{\chi_1^0} - M_{\chi_1^\pm}$ plane from the ATLAS search for trileptons [16] (assuming heavy sleptons) have been obtained using the simplified detector simulation DELPHES [66, 67]; this simulation should actually be redone by the LHC collaborations themselves. In any case it shows that the signal rates in this scenario are measurably large, and that relevant constraints are obtained in the absence of signals.

In addition to the trilepton final state, the simplified higgsino-singlino scenario can also be tested in searches for four leptons plus E_T^{miss} [17, 70]. The relevant processes would be $pp \rightarrow Z^* \rightarrow \chi_i^0 \chi_j^0$ with $i, j = 2, 3$, $\chi_{i,j}^0 \rightarrow \chi_1^0 + Z^{(*)}$ and leptonic decays of $Z^{(*)}$ (or, alternatively, hadronic decays of one of the $Z^{(*)}$ [17, 71]). Again, the masses and mixing angles given here allow for the determination of the production cross sections. These are dominated by $\chi_2^0 + \chi_3^0$ production with, however, a cross section of only $\sim 20 - 25\%$ of the one for trileptons. At present, the results of these searches are interpreted in SUSY models with gauge mediation where χ_1^0 is replaced by a practically massless gravitino. Hence, re-analyses of these (and future) results are desirable in the context of the present scenario.

In how far does this simplified light higgsino-singlino scenario differ from more general regions in the parameter space of the NMSSM? First, if the wino mass parameter M_2 is not as large as assumed here (2 TeV), the lightest chargino and neutralinos can have sizeable wino components which lead typically to an increase of the production cross sections. Hence the present scenario is conservative in this respect. On the other hand, the neutralinos $\chi_{2,3}^0$ will not necessarily have branching ratios of 100% into $Z^{(*)} + \chi_1^0$, notably if decays into some of the lighter of the 5 CP-even or CP-odd neutral Higgs states of the NMSSM are frequent. Clearly such decays would reduce the signal rate in the trilepton channel considered here – even if $\chi_{2,3}^0$ decay into a light pseudoscalar A_1 with $M_{A_1} < 2M_b$ and A_1 decays dominantly into $A_1 \rightarrow \tau^+ \tau^-$ [72, 73]. Decays of $\chi_{2,3}^0$ into heavier Higgs states (decaying into $b\bar{b}$), however, start also to be constrained by corresponding searches [74]. Implications of these latter results on more general regions in the parameter space of the NMSSM remain to be worked out.

Acknowledgements

It is a pleasure to thank A. Teixeira for discussions. We acknowledge support from the French ANR LFV-CPV-LHC, the European Union FP7 ITN INVISIBLES (Marie Curie Actions, PITN-GA-2011-289442) and the ERC advanced grant Higgs@LHC.

Appendix

Below we list in the form of Tables in the $M_{\chi_1^0} - M_{\chi_1^\pm}$ plane various parameters relevant for the simplified light higgsino-singlino scenario in the NMSSM. First, in Table 1 we show the values of μ_{eff} leading to specific values for $M_{\chi_1^\pm}$ (which do not depend on $M_{\chi_1^0}$). In Table 2 we give the values of κ which lead to the corresponding values of $M_{\chi_1^0}$. In the Tables 3 and 4 we list $M_{\chi_2^0}$ and $M_{\chi_3^0}$, and in the Tables 5, 6, 7 and 8 we list $N_{2,3}$, $N_{2,4}$, $N_{3,3}$ and $N_{3,4}$, respectively.

$M_{\chi_1^\pm}$	100.0	120.0	140.0	160.0	180.0	200.0	220.0	240.0	260.0	280.0	300.0	320.0	340.0	360.0	380.0	400.0
μ_{eff}	99.3	118.8	138.4	157.9	177.5	197.2	216.8	236.5	256.1	275.8	295.6	315.3	335.0	354.8	374.6	394.3

Table 1: Values for μ_{eff} leading to the specific values of $M_{\chi_1^\pm}$ used below.

$M_{\chi_1^\pm}$:	100.0	120.0	140.0	160.0	180.0	200.0	220.0	240.0	260.0	280.0	300.0	320.0	340.0	360.0	380.0	400.0
$M_{\chi_1^0}$	κ															
0	-.242	-.170	-.126	-.097	-.077	-.063	-.052	-.044	-.037	-.032	-.028	-.025	-.022	-.020	-.018	-.016
10	-.185	-.129	-.095	-.072	-.056	-.044	-.036	-.029	-.024	-.020	-.017	-.015	-.013	-.011	-.009	-.008
20	-.130	-.090	-.064	-.047	-.035	-.026	-.020	-.015	-.011	-.008	-.006	-.004	-.003	-.002	-.001	-.000
30	-.077	-.051	-.034	-.022	-.014	-.008	-.004	-.089	0.002	0.003	0.005	0.006	0.006	0.007	0.007	0.008
40	-.025	-.013	-.004	0.003	0.007	0.010	0.012	0.014	0.015	0.015	0.016	0.016	0.016	0.016	0.016	0.016
50	0.029	0.025	0.026	0.027	0.028	0.028	0.028	0.028	0.027	0.027	0.026	0.026	0.025	0.025	0.024	0.023
60	0.088	0.064	0.055	0.051	0.048	0.046	0.044	0.042	0.040	0.039	0.037	0.036	0.035	0.033	0.032	0.031
70	0.159	0.105	0.086	0.075	0.068	0.063	0.059	0.056	0.053	0.050	0.048	0.046	0.044	0.042	0.041	0.039
80	0.264	0.151	0.117	0.100	0.089	0.081	0.075	0.070	0.066	0.062	0.059	0.056	0.053	0.051	0.049	0.047
90	0.539	0.207	0.150	0.125	0.110	0.099	0.091	0.084	0.079	0.074	0.070	0.066	0.063	0.060	0.057	0.055
100	—	0.293	0.188	0.152	0.131	0.117	0.107	0.098	0.091	0.086	0.080	0.076	0.072	0.069	0.066	0.063

Table 2: κ as function of $M_{\chi_1^0}$ and $M_{\chi_1^\pm}$.

$M_{\chi_1^\pm}$:	100.0	120.0	140.0	160.0	180.0	200.0	220.0	240.0	260.0	280.0	300.0	320.0	340.0	360.0	380.0	400.0
$M_{\chi_1^0}$	$M_{\chi_2^0}$															
0	105.9	125.1	144.4	163.7	183.2	202.7	222.3	241.9	261.5	281.2	300.9	320.6	340.3	360.1	379.9	399.7
10	107.1	125.9	145.0	164.2	183.5	203.0	222.5	242.1	261.7	281.4	301.0	320.7	340.5	360.2	379.9	399.7
20	108.5	126.9	145.7	164.7	184.0	203.3	222.8	242.3	261.9	281.5	301.2	320.9	340.6	360.3	380.0	399.8
30	110.4	128.1	146.5	165.3	184.4	203.7	223.0	241.3	262.1	281.7	301.3	321.0	340.7	360.4	380.1	399.9
40	112.8	129.6	147.5	166.0	184.9	204.1	223.4	242.8	262.3	281.9	301.5	321.1	340.8	360.5	380.3	399.9
50	116.3	131.5	148.7	166.9	185.6	204.6	223.7	243.1	262.5	282.1	301.6	321.3	340.9	360.6	380.4	400.1
60	121.7	134.0	150.2	167.9	186.3	205.1	224.1	243.4	262.8	282.3	301.8	321.4	341.1	360.7	380.5	400.1
70	130.9	137.7	152.2	169.1	187.1	205.7	224.6	243.8	263.1	282.5	302.0	321.6	341.2	360.9	380.5	400.2
80	-145.5	143.2	154.8	170.6	188.1	206.4	225.1	244.2	263.4	282.8	302.3	321.8	341.4	361.0	380.7	400.3
90	-134.4	152.7	158.5	172.6	189.3	207.2	225.7	244.6	263.8	283.1	302.5	322.0	341.5	361.1	380.8	400.5
100	—	-158.9	164.1	175.2	190.9	208.2	226.5	245.2	264.2	283.4	302.8	322.2	341.7	361.3	380.9	400.6

Table 3: $M_{\chi_2^0}$ as function of $M_{\chi_1^0}$ and $M_{\chi_1^\pm}$.

$M_{\chi_1^\pm}$:	100.0	120.0	140.0	160.0	180.0	200.0	220.0	240.0	260.0	280.0	300.0	320.0	340.0	360.0	380.0	400.0
$M_{\chi_1^0}$	$-M_{\chi_3^0}$															
0	194.2	200.2	210.0	222.1	235.9	250.9	266.8	283.4	300.4	317.9	335.7	353.7	372.0	390.5	409.2	428.0
10	185.8	194.3	205.5	218.7	233.2	248.7	264.9	281.8	299.1	316.7	334.7	352.9	371.3	389.8	408.5	427.4
20	178.5	189.0	201.6	215.6	230.7	246.6	263.2	280.3	297.8	315.6	333.7	352.0	370.5	389.1	407.9	426.8
30	172.3	184.5	198.0	212.8	228.4	244.8	261.6	289.0	296.6	314.6	332.8	351.2	369.8	388.5	407.3	426.3
40	166.7	180.4	194.9	210.3	226.3	243.0	260.1	277.7	295.5	313.6	331.9	350.4	369.1	387.9	406.8	425.8
50	161.6	176.7	192.0	208.0	224.4	241.4	258.8	276.5	294.5	312.7	331.1	349.7	368.4	387.3	406.3	425.3
60	156.8	173.3	189.4	205.8	222.7	239.9	257.5	275.4	293.5	311.8	330.4	349.0	367.8	386.7	405.8	424.8
70	151.7	170.0	186.9	203.9	221.0	238.5	256.3	274.3	292.6	311.0	329.6	348.4	367.2	386.2	405.3	424.4
80	-150.7	166.8	184.6	202.0	219.5	237.2	255.2	273.4	291.7	310.3	329.0	347.7	366.7	385.7	404.8	423.9
90	-223.5	163.3	182.4	200.3	218.1	236.0	254.1	272.4	290.9	309.5	328.3	347.1	366.1	385.2	404.3	423.6
100	—	-173.2	180.1	198.6	216.7	234.9	253.1	271.6	290.1	308.8	327.7	346.6	365.6	384.7	403.9	423.1

Table 4: $-M_{\chi_3^0}$ as function of $M_{\chi_1^0}$ and $M_{\chi_1^\pm}$. (The negative sign is chosen only to keep the linewidths reasonably short.)

$M_{\chi_1^\pm}$:	100	120	140	160	180	200	220	240	260	280	300	320	340	360	380	400
$M_{\chi_1^0}$	$N_{2,3}$															
0	.764	.751	.742	.735	.730	.726	.723	.720	.719	.717	.716	.714	.713	.713	.712	.711
10	.767	.753	.743	.736	.730	.726	.723	.721	.719	.717	.716	.715	.714	.713	.712	.711
20	.770	.754	.744	.736	.731	.727	.724	.721	.719	.717	.716	.715	.714	.713	.712	.711
30	.770	.755	.745	.737	.731	.727	.724	.720	.719	.717	.716	.715	.714	.713	.712	.711
40	.768	.755	.745	.738	.732	.727	.724	.721	.719	.718	.716	.715	.714	.713	.712	.711
50	.758	.753	.745	.738	.732	.728	.724	.722	.719	.718	.716	.715	.714	.713	.712	.712
60	.736	.747	.743	.737	.732	.728	.724	.722	.720	.718	.716	.715	.714	.713	.712	.712
70	.689	.734	.739	.736	.732	.728	.724	.722	.720	.718	.716	.715	.714	.713	.712	.712
80	.687	.707	.731	.733	.730	.727	.724	.722	.720	.718	.716	.715	.714	.713	.712	.712
90	.700	.653	.715	.727	.728	.726	.724	.722	.720	.718	.717	.715	.714	.713	.712	.712
100	—	.690	.685	.717	.725	.725	.723	.721	.720	.718	.717	.715	.714	.713	.712	.712

Table 5: $N_{2,3}$ as function of $M_{\chi_1^0}$ and $M_{\chi_1^\pm}$.

$M_{\chi_1^\pm}$:	100	120	140	160	180	200	220	240	260	280	300	320	340	360	380	400
$M_{\chi_1^0}$	$N_{2,4}$															
0	-.600	-.623	-.640	-.652	-.661	-.668	-.674	-.678	-.682	-.684	-.687	-.689	-.690	-.691	-.692	-.693
10	-.583	-.613	-.633	-.647	-.658	-.666	-.672	-.677	-.680	-.683	-.686	-.688	-.690	-.691	-.692	-.693
20	-.562	-.600	-.625	-.642	-.654	-.663	-.670	-.675	-.679	-.682	-.685	-.687	-.689	-.691	-.692	-.693
30	-.535	-.585	-.615	-.636	-.650	-.660	-.668	-.682	-.678	-.681	-.684	-.687	-.688	-.690	-.691	-.692
40	-.499	-.565	-.604	-.628	-.645	-.656	-.665	-.671	-.676	-.680	-.683	-.686	-.688	-.689	-.691	-.692
50	-.450	-.540	-.589	-.619	-.639	-.652	-.662	-.669	-.675	-.679	-.682	-.685	-.687	-.689	-.690	-.692
60	-.380	-.506	-.571	-.608	-.632	-.647	-.659	-.667	-.673	-.677	-.681	-.684	-.686	-.688	-.690	-.691
70	.279	-.459	-.546	-.594	-.623	-.642	-.655	-.664	-.671	-.676	-.680	-.683	-.686	-.688	-.689	-.691
80	.616	-.391	-.513	-.576	-.612	-.635	-.650	-.661	-.668	-.674	-.678	-.682	-.685	-.687	-.689	-.690
90	.648	-.294	-.468	-.553	-.599	-.627	-.645	-.657	-.665	-.672	-.677	-.681	-.684	-.686	-.688	-.690
100	—	.640	-.402	-.521	-.582	-.616	-.638	-.652	-.662	-.670	-.675	-.679	-.683	-.685	-.687	-.689

Table 6: $N_{2,4}$ as function of $M_{\chi_1^0}$ and $M_{\chi_1^\pm}$.

$M_{\chi_1^\pm}$:	100	120	140	160	180	200	220	240	260	280	300	320	340	360	380	400
$M_{\chi_1^0}$	$N_{3,3}$															
0	.571	.600	.621	.636	.648	.658	.665	.671	.675	.679	.683	.685	.687	.689	.691	.693
10	.591	.614	.632	.645	.655	.662	.669	.674	.678	.681	.684	.687	.689	.690	.692	.693
20	.609	.627	.641	.652	.660	.667	.672	.677	.680	.683	.686	.688	.690	.691	.693	.694
30	.625	.638	.649	.658	.665	.671	.675	.659	.682	.685	.687	.689	.691	.692	.694	.695
40	.638	.648	.656	.663	.669	.674	.678	.681	.684	.686	.689	.690	.692	.693	.694	.695
50	.650	.656	.662	.668	.673	.677	.680	.683	.686	.688	.690	.691	.693	.694	.695	.696
60	.661	.663	.668	.672	.676	.680	.683	.685	.687	.689	.691	.692	.693	.695	.696	.696
70	.672	.670	.673	.676	.679	.682	.685	.687	.689	.690	.692	.693	.694	.695	.696	.697
80	.583	.676	.677	.679	.682	.684	.686	.688	.690	.691	.693	.694	.695	.696	.697	.697
90	.374	.683	.681	.682	.684	.686	.688	.690	.691	.692	.694	.695	.696	.696	.697	.698
100	—	.548	.685	.685	.686	.688	.689	.691	.692	.693	.694	.695	.696	.697	.698	.698

Table 7: $N_{3,3}$ as function of $M_{\chi_1^0}$ and $M_{\chi_1^\pm}$.

$M_{\chi_1^\pm}$:	100	120	140	160	180	200	220	240	260	280	300	320	340	360	380	400
$M_{\chi_1^0}$	$N_{3,4}$															
0	.468	.515	.550	.578	.600	.616	.630	.641	.649	.657	.662	.667	.672	.675	.678	.681
10	.492	.533	.564	.589	.608	.623	.635	.645	.653	.659	.665	.669	.673	.677	.680	.682
20	.513	.549	.576	.598	.615	.629	.640	.648	.656	.662	.667	.671	.675	.678	.681	.683
30	.532	.563	.587	.606	.622	.634	.644	.625	.659	.664	.669	.673	.676	.679	.682	.684
40	.549	.575	.597	.614	.627	.639	.648	.655	.661	.666	.671	.675	.678	.681	.683	.685
50	.565	.587	.605	.620	.633	.643	.651	.658	.664	.668	.673	.676	.679	.682	.684	.686
60	.581	.597	.613	.626	.638	.647	.654	.661	.666	.670	.674	.677	.680	.683	.685	.687
70	.597	.607	.620	.632	.642	.650	.657	.663	.668	.672	.676	.679	.681	.684	.686	.687
80	-.137	.617	.627	.637	.646	.654	.660	.665	.670	.674	.677	.680	.682	.685	.686	.688
90	.252	.627	.633	.642	.650	.657	.662	.667	.672	.675	.678	.681	.683	.685	.687	.689
100	—	.155	.640	.646	.653	.659	.665	.669	.673	.677	.680	.682	.684	.686	.688	.689

Table 8: $N_{3,4}$ as function of $M_{\chi_1^0}$ and $M_{\chi_1^\pm}$.

References

- [1] P. Nath and R. L. Arnowitt, *Mod. Phys. Lett. A* **2** (1987) 331.
- [2] R. L. Arnowitt, R. M. Barnett, P. Nath and F. Paige, *Int. J. Mod. Phys. A* **2** (1987) 1113.
- [3] R. Barbieri, F. Caravaglios, M. Frigeni and M. L. Mangano, *Nucl. Phys. B* **367** (1991) 28.
- [4] H. Baer and X. Tata, *Phys. Rev. D* **47** (1993) 2739.
- [5] J. L. Lopez, D. V. Nanopoulos, X. Wang and A. Zichichi, *Phys. Rev. D* **48** (1993) 2062 [hep-ph/9211286].
- [6] H. Baer, C. Kao and X. Tata, *Phys. Rev. D* **48** (1993) 5175 [hep-ph/9307347].
- [7] H. Baer, C. H. Chen, F. Paige and X. Tata, *Phys. Rev. D* **50** (1994) 4508 [hep-ph/9404212].
- [8] H. Baer, C. H. Chen, F. Paige and X. Tata, *Phys. Rev. D* **53** (1996) 6241 [hep-ph/9512383].
- [9] H. Baer, V. Barger, S. Kraml, A. Lessa, W. Sreethawong and X. Tata, *JHEP* **1203** (2012) 092 [arXiv:1201.5382 [hep-ph]].
- [10] [CMS Collaboration], *JHEP* **06** (2012) 169, doi:10.1007/JHEP06(2012)169.
- [11] ATLAS Collaboration, ATLAS-CONF-2012-154, <http://cdsweb.cern.ch/record/1493493>
- [12] G. Aad *et al.* [ATLAS Collaboration], *Phys. Rev. Lett.* **108** (2012) 261804 [arXiv:1204.5638 [hep-ex]].
- [13] G. Aad *et al.* [ATLAS Collaboration], *Phys. Lett. B* **718** (2013) 841 [arXiv:1208.3144 [hep-ex]].
- [14] S. Chatrchyan *et al.* [CMS Collaboration], *JHEP* **1211** (2012) 147 [arXiv:1209.6620 [hep-ex]].
- [15] [CMS Collaboration] “Search for electroweak production of charginos, neutralinos, and sleptons using leptonic final states in pp collisions at $\sqrt{s} = 8$ TeV,” CMS-PAS-SUS-12-022.
- [16] [ATLAS Collaboration], “Search for direct production of charginos and neutralinos in events with three leptons and missing transverse momentum in 21 fb^{-1} of pp collisions at $\sqrt{s} = 8$ TeV with the ATLAS detector,” ATLAS-CONF-2013-035.
- [17] [CMS Collaboration] “Search for electroweak production of charginos, neutralinos, and sleptons using leptonic final states in pp collisions at $\sqrt{s} = 8$ TeV,” CMS-PAS-SUS-13-006

- [18] S. S. AbdusSalam, Phys. Rev. D **87** (2013) 115012 [arXiv:1211.0999 [hep-ph]].
- [19] A. Bharucha, S. Heinemeyer and F. von der Pahlen, “Direct Chargino-Neutralino Production at the LHC: Interpreting the Exclusion Limits in the Complex MSSM,” arXiv:1307.4237 [hep-ph].
- [20] K. Kowalska and E. M. Sessolo, “Natural MSSM after the LHC 8 TeV run,” arXiv:1307.5790 [hep-ph].
- [21] G. Belanger, G. D. La Rochelle, B. Dumont, R. M. Godbole, S. Kraml and S. Kulkarni, “LHC constraints on light neutralino dark matter in the MSSM,” arXiv:1308.3735 [hep-ph].
- [22] M. Frank, L. Selbuz and I. Turan, “Neutralino and Chargino Production in U(1)’ at the LHC,” arXiv:1212.4428 [hep-ph].
- [23] T. Cheng, J. Li, T. Li and Q. -S. Yan, “Natural NMSSM confronting with the LHC7-8,” arXiv:1304.3182 [hep-ph].
- [24] A. Alloul, M. Frank, B. Fuks and M. R. de Trautenberg, “Chargino and neutralino production at the Large Hadron Collider in left-right supersymmetric models,” arXiv:1307.5073 [hep-ph].
- [25] H. Baer, V. Barger and P. Huang, JHEP **1111** (2011) 031 [arXiv:1107.5581 [hep-ph]].
- [26] S. Bobrovskiy, F. Brummer, W. Buchmuller and J. Hajer, JHEP **1201** (2012) 122 [arXiv:1111.6005 [hep-ph]].
- [27] M. Perelstein and B. Shakya, JHEP **1110** (2011) 142 [arXiv:1107.5048 [hep-ph]].
- [28] E. Aprile *et al.* [XENON100 Collaboration], Phys. Rev. Lett. **109** (2012) 181301 [arXiv:1207.5988 [astro-ph.CO]].
- [29] U. Ellwanger, C. Hugonie and A. M. Teixeira, Phys. Rept. **496** (2010) 1 [arXiv:0910.1785 [hep-ph]].
- [30] U. Ellwanger, G. Espitalier-Noel and C. Hugonie, JHEP **1109** (2011) 105 [arXiv:1107.2472 [hep-ph]].
- [31] M. Perelstein and B. Shakya, “XENON100 Implications for Naturalness in the MSSM, NMSSM and lambda-SUSY,” arXiv:1208.0833 [hep-ph].
- [32] D. G. Cerdeno, C. Hugonie, D. E. Lopez-Fogliani, C. Munoz and A. M. Teixeira, JHEP **0412** (2004) 048 [hep-ph/0408102].
- [33] D. G. Cerdeno, E. Gabrielli, D. E. Lopez-Fogliani, C. Munoz and A. M. Teixeira, JCAP **0706** (2007) 008 [hep-ph/0701271 [HEP-PH]].
- [34] V. Barger, P. Langacker, I. Lewis, M. McCaskey, G. Shaughnessy and B. Yencho, Phys. Rev. D **75** (2007) 115002 [hep-ph/0702036 [HEP-PH]].

- [35] G. Belanger, C. Hugonie and A. Pukhov, JCAP **0901** (2009) 023 [arXiv:0811.3224 [hep-ph]].
- [36] L. J. Hall, D. Pinner and J. T. Ruderman, JHEP **1204** (2012) 131 [arXiv:1112.2703 [hep-ph]].
- [37] U. Ellwanger, JHEP **1203** (2012) 044 [arXiv:1112.3548 [hep-ph]].
- [38] A. Arvanitaki and G. Villadoro, JHEP **1202** (2012) 144 [arXiv:1112.4835 [hep-ph]].
- [39] S. F. King, M. Muhlleitner and R. Nevzorov, Nucl. Phys. B **860** (2012) 207 [arXiv:1201.2671 [hep-ph]].
- [40] Z. Kang, J. Li and T. Li, JHEP **1211** (2012) 024 [arXiv:1201.5305 [hep-ph]].
- [41] J. -J. Cao, Z. -X. Heng, J. M. Yang, Y. -M. Zhang and J. -Y. Zhu, JHEP **1203** (2012) 086 [arXiv:1202.5821 [hep-ph]].
- [42] U. Ellwanger and C. Hugonie, Adv. High Energy Phys. **2012** (2012) 625389 [arXiv:1203.5048 [hep-ph]].
- [43] K. S. Jeong, Y. Shoji and M. Yamaguchi, JHEP **1209** (2012) 007 [arXiv:1205.2486 [hep-ph]].
- [44] L. Randall and M. Reece, JHEP **1308** (2013) 088 [arXiv:1206.6540 [hep-ph]].
- [45] R. Benbrik, M. Gomez Bock, S. Heinemeyer, O. Stal, G. Weiglein and L. Zeune, Eur. Phys. J. C **72** (2012) 2171 [arXiv:1207.1096 [hep-ph]].
- [46] B. Kyae and J. -C. Park, Phys. Rev. D **87** (2013) 075021
- [47] J. Cao, Z. Heng, J. M. Yang and J. Zhu, JHEP **1210** (2012) 079 [arXiv:1207.3698 [hep-ph]].
- [48] K. Agashe, Y. Cui and R. Franceschini, JHEP **1302** (2013) 031 [arXiv:1209.2115 [hep-ph]].
- [49] G. Belanger, U. Ellwanger, J. F. Gunion, Y. Jiang, S. Kraml and J. H. Schwarz, JHEP **1301** (2013) 069 [arXiv:1210.1976 [hep-ph]].
- [50] Z. Heng, “A 125 GeV Higgs and its di-photon signal in different Susy models: a mini review,” arXiv:1210.3751 [hep-ph].
- [51] K. Choi, S. H. Im, K. S. Jeong and M. Yamaguchi, JHEP **1302** (2013) 090 [arXiv:1211.0875 [hep-ph]].
- [52] S. F. King, M. Muhlleitner, R. Nevzorov and K. Walz, Nucl. Phys. B **870** (2013) 323 [arXiv:1211.5074 [hep-ph]].
- [53] T. Gherghetta, B. von Harling, A. D. Medina and M. A. Schmidt, JHEP **1302** (2013) 032 [JHEP **1302** (2013) 032] [arXiv:1212.5243 [hep-ph]].

- [54] R. Barbieri, D. Buttazzo, K. Kannike, F. Sala and A. Tesi, Phys. Rev. D **87** (2013) 115018 [arXiv:1304.3670 [hep-ph]].
- [55] M. Badziak, M. Olechowski and S. Pokorski, JHEP **1306** (2013) 043 [arXiv:1304.5437 [hep-ph]].
- [56] T. Cheng and T. Li, Phys. Rev. D **88** (2013) 015031 [arXiv:1305.3214 [hep-ph]].
- [57] E. Hardy, “Is Natural Susy Natural?,” arXiv:1306.1534 [hep-ph].
- [58] C. Beskidt, W. de Boer and D. I. Kazakov, “A comparison of the Higgs sectors of the MSSM and NMSSM for a 126 GeV Higgs boson,” arXiv:1308.1333 [hep-ph].
- [59] U. Ellwanger, J. F. Gunion and C. Hugonie, JHEP **0502** (2005) 066 [arXiv:hep-ph/0406215].
- [60] U. Ellwanger and C. Hugonie, Comput. Phys. Commun. **175** (2006) 290 [arXiv:hep-ph/0508022], <http://www.th.u-psud.fr/NMHDECAY/nmssmtools.html>
- [61] W. Beenakker, R. Hopker, M. Spira and P. M. Zerwas, Nucl. Phys. B **492** (1997) 51 [arXiv:hep-ph/9610490].
- [62] W. Beenakker, R. Hopker and M. Spira, “PROSPINO: A program for the PROduction of Supersymmetric Particles In Next-to-leading Order QCD,” arXiv:hep-ph/9611232, for updates see <http://www.thphys.uni-heidelberg.de/~plehn/prospino/>
- [63] W. Beenakker, M. Klasen, M. Kramer, T. Plehn, M. Spira and P. M. Zerwas, Phys. Rev. Lett. **83** (1999) 3780 [Erratum-ibid. **100** (2008) 029901] [arXiv:hep-ph/9906298].
- [64] J. Alwall, M. Herquet, F. Maltoni, O. Mattelaer and T. Stelzer, JHEP **1106** (2011) 128 [arXiv:1106.0522 [hep-ph]].
- [65] T. Sjostrand, S. Mrenna and P. Z. Skands, JHEP **0605** (2006) 026 [hep-ph/0603175].
- [66] S. Ovin, X. Rouby and V. Lemaître, “DELPHES, a framework for fast simulation of a generic collider experiment,” arXiv:0903.2225 [hep-ph].
- [67] J. de Favereau, C. Delaere, P. Demin, A. Giammanco, V. Lemaître, A. Mertens and M. Selvaggi, “DELPHES 3, A modular framework for fast simulation of a generic collider experiment,” arXiv:1307.6346 [hep-ex].
- [68] J. Abdallah *et al.* [DELPHI Collaboration], Eur. Phys. J. C **31** (2003) 421 [hep-ex/0311019].
- [69] G. Abbiendi *et al.* [OPAL Collaboration], Eur. Phys. J. C **35** (2004) 1 [hep-ex/0401026].
- [70] [ATLAS Collaboration], “Search for supersymmetry in events with four or more leptons in 21 fb⁻¹ of pp collisions at $\sqrt{s} = 8$ TeV with the ATLAS detector,” ATLAS-CONF-2013-036.

- [71] [ATLAS Collaboration], “Search for supersymmetry in final states with jets, missing transverse momentum and a Z boson at $\sqrt{s} = 8$ TeV with the ATLAS detector,” ATLAS-CONF-2012-152.
- [72] K. Cheung and T. -J. Hou, Phys. Lett. B **674** (2009) 54 [arXiv:0809.1122 [hep-ph]].
- [73] D. G. Cerdeno, P. Ghosh, C. B. Park and M. Peiro, “Collider signatures of a light NMSSM pseudoscalar in neutralino decays in the light of LHC results,” arXiv:1307.7601 [hep-ph].
- [74] [CMS Collaboration] “Search for electroweak production of charginos and neutralinos in final states with a Higgs boson in pp collisions at $\sqrt{s} = 8$ TeV,” CMS-PAS-SUS-13-017.